An Overview of Methods and a New 3D FEA and Analytical Hybrid Technique for Calculating AC Winding Losses in PM Machines

Narges Taran, *Member, IEEE*, Dan M. Ionel, *Fellow, IEEE*, Vandana Rallabandi, *Senior Member, IEEE*, Greg Heins, *Member, IEEE*, and Dean Patterson, *Life Fellow, IEEE*

***Abstract*—This paper proposes a new hybrid analytical and numerical finite element (FE) based method for calculating ac eddy current losses in wire windings and demonstrates its applicability for axial flux permanent magnet electric machines. The method takes into account 3D field effects in order to achieve accurate results and yet greatly reduce computational efforts. The new 3D FE-based method is advantageous as it employs minimum simplifications and considers the end turns in the eddy current path, the magnetic flux density variation along the effective length of coils, and the field fringing and leakage, which ultimately increases the accuracy of simulations. This study is one of the first ones to compare meticulous 3D finite element analysis (FEA) models with more approximate, but faster solution methods which can be employed in the optimization process. The accuracy of the 3D FEA calculations have been confirmed through tests on a prototype axial flux permanent magnet machine. The proposed method is applicable for cases with majority of ac copper losses induced due to external magnetic flux sources, such as permanent magnets. Examples of such machines designs are coreless or open slot PM machines with conductors sizes smaller than skin depth.**

***Index Terms*—Eddy current loss, ac winding loss, finite element, 3D model, PM machine, axial flux motor.**

I. Introduction

The accurate prediction of the power loss components plays a vital role in the effective optimal design of electric machines, and, in this respect, ac eddy current winding losses are very important, especially in high-speed and high-power density designs. In this case, the nonlinearity caused by the large magnetic loading may increase the slot opening flux leakage and result into winding losses even at open circuit in addition to increased losses due to the proximity effects at load operation [1]–[3]. Some of the concerns related to the design of electric machines with reduced additional ac copper loss have been addressed for example in [4], [5].

Several authors have analytically estimated the additional ac copper loss [6]–[13]. Analytical methods are more straightforward to use, but typically employ many simplifying assumptions, leading to approximate results. Numerical techniques, such as finite element analysis (FEA), may be more accurate with the downside of a laborious set-up process and substantial computer resource requirements. Two–dimensional FEA is used in many studies [2], [5], [14], [15] while 3D FEA has been employed only very recently in few works [16], [17]. Hybrid methods for the estimation of skin and proximity effect losses are also investigated in [3], [18], [19].

These hybrid methods generally employ the FEA calculated flux density in one coil cross section in order to provide a trade-off between accuracy and computational speed. On the other hand, due to end effects, flux leakage and fringing, the flux density observed by the winding in different cross sections may not be identical and hence employing a 2D FEA model may not suffice. For machines with considerable flux leakage at the ends, hybrid methods that utilize 2D finite element (FE) models can overestimate the losses. Additionally, the accuracy is negatively affected because 2D models cannot take into account the end path of the eddy currents. The possible problems associated with sampling the flux density from a 2D FE model are discussed in more detail later in the paper. Furthermore, it should be noted that electrical machines, such as those of the axial flux type, in which the flux density in the slots and winding conductors vary both in the axial and radial directions, have a substantially three dimensional magnetic flux path and require adequate 3D FE models.

This paper is a follow-up expansion of the conference papers [20] and [21], and proposes a new hybrid method with minimal simplifying assumptions. The proposed method is applicable for cases where proximity losses due to adjacent conductors are a smaller portion of overall ac component of copper losses. This is usually the case for lower frequency machines, coils with thinner dimension compared to skin depth, coreless, or open slot PM machines. The proposed method is particularly beneficial for radial flux PM machines with shorter stack length and axial flux PM machines with larger split ratios (the ratio of inner to outer diameter).

The analytical formulation is derived with the corresponding equations and the results are compared with meticulous 3D FEA of models with the windings detailed wire-by-wire. The method is illustrated along with more conventional approaches on example axial flux permanent magnet (AFPM) machines with concentrated coils around the teeth and open slots, and with a coreless stator structure, respectively. The additional

N. Taran and V. Rallabandi were with the SPARK Laboratory Department of Electrical and Computer Engineering, University of Kentucky, Lexington, KY 40506 USA and they are now with BorgWarner Inc., Noblesville Technical Center, IN and with GE Research, Niskayuna, NY, respectively (e-mails: narges.taran@ieee.org and vandana.rallabandi@ieee.org). D. M. Ionel is with the SPARK Laboratory, Department of Electrical and Computer Engineering, University of Kentucky, Lexington, KY 40506 USA (e-mail: dan.ionel@ieee.org). G. Heins and D. Patterson are with the Regal Beloit Corporation, Australia, Rowville, VIC 3178, Australia (e-mails: greg.heins@regalbeloit.com; dean.patterson@regalbeloit.com).

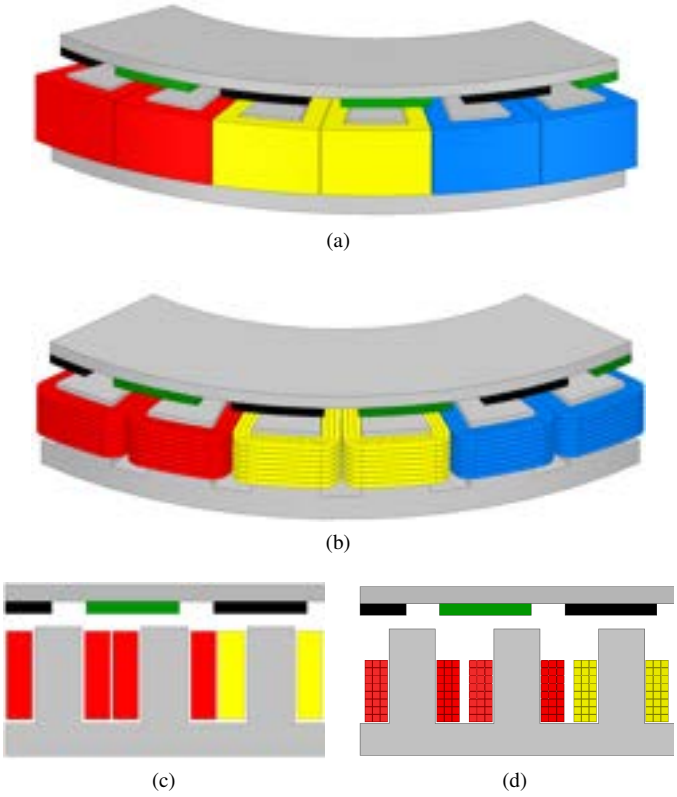

Fig. 1: The geometries employed for the FE models of the AFPM machine considered in the study. (a) Simplified 3D model with large equivalent single turn coil, (b) 3D model with turn-by-turn representation of wire conductors, (c) simplified 2D model with large equivalent single turn coil, and (d) 2D model with detailed turn-by-turn representation of the wire conductors.

conductor loss caused by rotor PMs is significant in case of open slot machines, due to the increased leakage flux, and an extreme case occurs for air cored machines where the stator core is eliminated and all conductors are exposed to the air gap flux density.

The following section describes the validation of 3D FEA based conductor ac current loss calculation with measurements on a prototype machine. Section III presents a review of the existing conductor ac loss calculation methods. The proposed hybrid method is introduced in section IV, and its application for air cored and open slot AFPM machines are discussed in section V. The study concludes in section VI.

II. Experimental and 3D FEA Validation Study on a Special Prototype

The experimental validation of detailed 3D FEA, which is employed later in the paper as a reference computational method, is performed for a special prototype AFPM machine with open slots and movable coils concentrated around the teeth. Conductors with a square cross section, as shown in Fig. 1, are employed in order to facilitate construction.

Four types of geometries for the FEA modeling of the prototype AFPM machine are shown in Fig. 1. These include 2D and 3D models with a general large equivalent single turn coil, Figs 1a and 1c, and detailed turn-by-turn models of the conductors, Figs. 1b and 1d. The proximity effects caused by the ac current flowing in adjacent conductors is ignored when the ac copper loss estimation relies on FEAs similar to Fig. 1a and Fig. 1c.

Throughout this study, the open slot cored AFPM design utilizes circular conductors with radius of 1 mm or square conductors 1.63×1.63 mm. The coreless design employs circular conductors with 0.25 mm radius. As it is a common practice, the wire dimensions are selected such that cross sectional dimensions are smaller than the skin depth. The analysis are done at max frequency of 1.6 kHz for cored AFPM machine which leads to skin depth of 1.7 mm. In the case of coreless machine the analysis are done at 480 Hz which results in skin depth of 3.2 mm. At higher frequencies, a Litz wire based design may be required, which is beyond the scope of the current paper.

Wire insulation is directly included in finite element models with turn-by-turn illustration. In case of crude models, the field is constrained within each conductor such that no additional losses are caused by neighbor conductors. ANSYS Electronics Desktop is employed to perform the electromagnetic finite element analysis [22].

The 3D FEA can be performed by meshing all the conductors or only the top conductors that are responsible for the majority of the losses, as illustrated in Fig. 2. With this approach of fine meshing only the conductors located closest to the airgap, the computational efforts can be reduced without significant impacts to the accuracy of the FEA results. Three-dimensional FEA results from Fig. 3 illustrate the current density and flux density in the conductors, confirming that the conductors closest to the airgap experience the highest magnetic fields and hence power loss. As it is shown later in Fig. 6, it has been ensured that coarse mesh of wires located deeper in the slot does not have adverse effects on the accuracy of the results.

An important point is that although the length of the mesh elements for the wires located deep in the slot are not very important, the mesh for the conductors closer to the slot opening should be assigned carefully and accurately. The length of mesh elements are assigned according to a mesh convergence study and taking the skin depth into account such that accurate estimation of copper losses is ensured.

The separation of loss components, particularly ac and dc copper losses involves special procedures, such as those described at [5], [14], [16], [23] . The proposed method for open-circuit copper loss estimation leverages its dependence on the distance of the coils to the outer surface of the rotor. The machine is operated in open-circuit, and power loss measurements are conducted. The open-circuit spinning loss includes the mechanical losses, such as friction and windage, stator core losses, copper losses due to PM field and losses in the PM. Spinning loss measurements are performed on the special motor prototype with two distinct coil placements that have different spacing from the rotor outer surface through the airgap. Numerical computations confirmed that with increasing spacing, the open-circuit eddy current winding copper loss

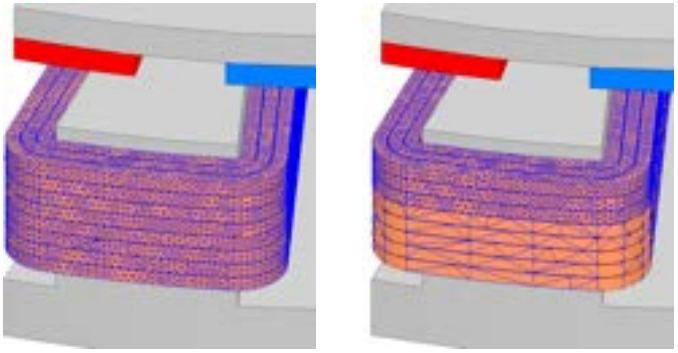

(a) (b)

Fig. 2: The 3D model of the prototype machine. The mesh can be fine for (a) all conductors or (b) only for the top conductors that cause the majority of open-circuit eddy current losses.

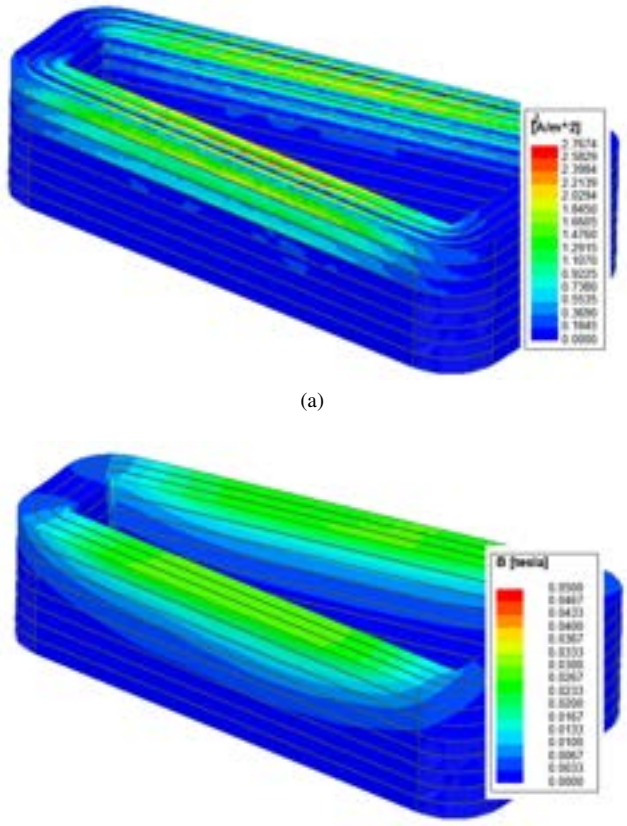

(a)

(b)

Fig. 3: Three-dimensional FEA results of the modeled prototype machine, operating at open-circuit and rated speed with fundamental frequency of 500 Hz, representing: (a) current density, and (b) flux density of the coils for the open slot AFPM machine case study.

reduces, ultimately becoming negligible for large spacings.

In a first set of experiments, the coils are placed closer to the rotor surface by inserting spaces in between the stator core and the coils as shown in Fig. 4. In a second set of experiments, the spacers are removed and the coils are placed at the very bottom of the slot, further away from the airgap and rotor, as

Fig. 4: The prototype machine with spacers.

Fig. 5: The prototype machine without spacers.

shown in Fig. 5. The size of the spacer is chosen to ensure that when removed, the coils are far enough away from the rotor surface that the eddy current losses are negligible. Another approach would be to use dummy coils such that no copper losses are included in this measurement. The spinning loss is measured in both experiments and the open-circuit ac copper loss is calculated as the difference between the results from the two tests.

The measurements are performed at different rotational speeds and the results presented in Fig. 6. The FEA estimations are in good agreement with measurement, particularly for the larger speeds where the loss value is larger and hence more feasible to measure. The time required to set up the detailed 3D model and run the FEA is very long, over 48 hours. This calls for a new method which can achieve accurate results with significant reduction in required time.

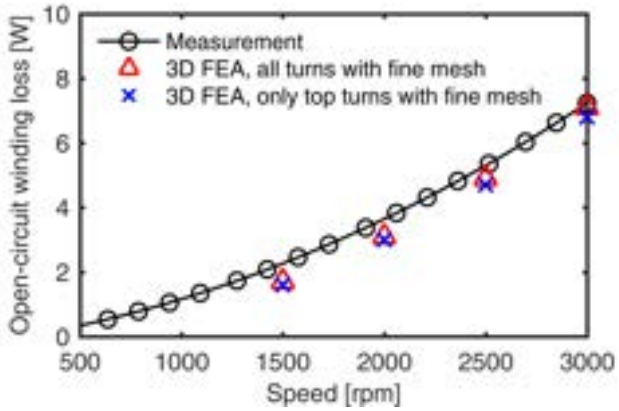

Fig. 6: The measurements of ac copper loss and validation of 3D FEA calculations.

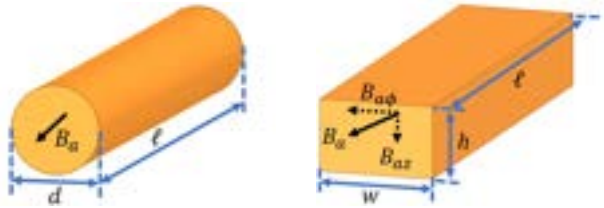

(a) (b)

Fig. 7: Illustration of wires with circular and rectangular cross section.

III. Methods for Calculating Eddy Current Losses

A. Analytical

The analytical methods for calculating eddy current loss, P_{eddy}, have been attempted in several publications. Majority of these approaches originate from the following

$$P_{eddy} = \frac{1}{R}\left(\frac{d\phi}{dt}\right)^2 , \tag{1}$$

where R is the resistance and ϕ is the magnetic flux seen by the conductors. It can be shown that for a machine with N_c coil sides with the length of ℓ, N_t turns per coil with circular cross section as shown in Fig. 7a, and N_s strands per turn with diameter of d, assuming no magnet flux leakage on the end coils and all of the coil region exposed to a space uniform flux density of B_a varying sinusoially in time, the eddy current loss can be estimated by

$$P_{eddy} = \frac{\pi \ell N_c N_t N_s d^4 B_a^2 \omega^2 \sigma}{128} , \tag{2}$$

where ω is the electrical angular speed and σ is the conductivity of the coil. Similarly, for the case with rectangular cross section conductors in Fig. 7b, these losses can be calculated as

$$P_{eddy} = \frac{\ell N_c N_t N_s w h \omega^2 \sigma}{24}(w^2 B_{az}^2 + h^2 B_{a\phi}^2) , \tag{3}$$

where B_{az} and $B_{a\phi}$ are the axial, in z direction, and tangential, in ϕ direction, component of the flux density as shown in Fig. 7b. The assumption of uniform B_a in many cases is not accurate due to skin effect, larger leakage flux at the top of the slots, circulating currents in parallel conductors, etc.

The accuracy of simple calculations such as (2) and (3), varies for different machine structures. For some topologies, such as air-cored machines with no over-hang, these estimations may be acceptable while for some other machines analytical approaches need to be implemented more carefully. For example, in machines where conductors are placed in slots, each turn experiences a different flux density. Also, if the conductor diameter is significantly larger than skin depth, the variation of B_a inside each turn is considerable. For instance, hairpin or bar windings cross section usually observe a range of flux density values at any given time.

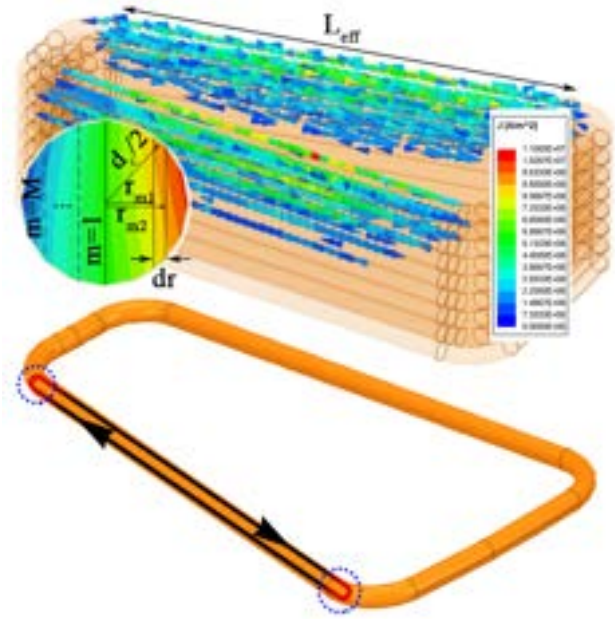

Fig. 8: Eddy current 3D distribution in the conductors (top) and a typical eddy current path considered in a 2D analysis, having a go and return path along the conductor L_{eff} and not including an end coil section.

B. Numerical Finite Element Analysis

It is possible to calculate the ac winding losses using numerical models, such as FEA. This requires to model the coils in detail, in a turn-by-turn and wire-by-wire approach. Therefore, this is a complicated task, difficult to parametrize and to employ in an optimization algorithm. The winding ac loss estimation requires fine meshing according to the skin depth, while the flux density can be estimated with a more coarse mesh.

Two-dimensional FEA is easier to set up and is faster, making it particularly suitable for large-scale parametric and optimization studies. However, a major disadvantage is that it cannot take into account the variations in the third dimension. On the other hand, 3D models can take end effects and 3D flux paths into account, but have the drawbacks of being laborious to set up and computationally expensive.

If all the conductors are modeled and meshed correctly considering the skin depth, the mesh size of the 3D turn-by-turn model would be very large (over 8 million elements in the case studies considered here). This necessitates use of high performance computing (HPC) systems and supercomputers. Another approach could be to fine mesh only the turns that cause the majority of the losses. For example and as shown in the previous section, for the open-slot AFPM machine most of these losses happen at the top three layers of the winding. Therefore, the rest of the turns can be meshed coarsely.

C. Hybrid Analytical–FEA Methods

Hybrid methods may provide, in principle, a satisfactory compromise between accuracy and computational efforts for estimating the ac eddy current component of copper losses. For such methods, a combination of analytical equations and

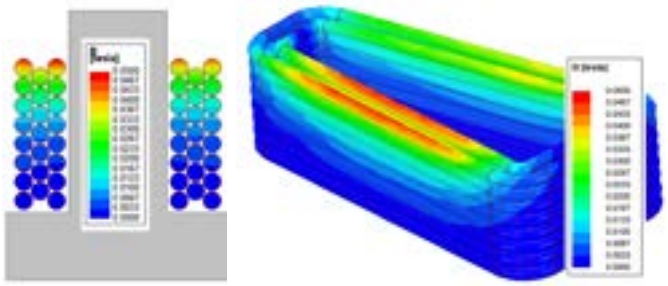

(a) (b)

Fig. 9: The magnetic flux density in the conductors of a concentrated precise wound coil placed in the slots of an example AFPM machine calculated with 2D (a) and 3D (b) FEA and illustrating the multi-dimensional variation of the field.

FEA is employed. Typically, flux density values are sampled from the simplified coil cross section representation of a 2D FE model, e.g. shown in Fig. 1c. The flux density is then used with analytical equations in order to calculate the eddy current losses.

Using crude coil for hybrid method significantely improves the FEA speed, however, it cannot take into account the distortion of current density due to neighboring conductors. Therefore, the proximity effects due to the adjacent wires or skin effect are not considered. The latter can be less significant if the wire size is smaller than the skin depth. In the case of coreless or open slot permanent magnet machines, where the majority of ac component of copper losses are due to PMs passing over the conductors, this approach can still lead to reasonable outcomes.

Although hybrid methods may lead to more accurate estimations than pure analytical methods, they have the risk of inaccuracy due to the fact that they disregard 3D effects. Neglecting end paths, as shown in Fig. 8 may result into underestimation of resistance and hence overestimation of eddy current losses. The end turn paths become a larger contributor to the resistance of the eddy current paths for shorter coils, i.e., lower stack length in case of radial flux machines or larger split ratio in case of axial flux machines. Therefore, it is necessary to consider the entire path of the eddy current loop. To do so, a correction factor is employed as:

$$K_s = 1 - \frac{\tanh\left(\frac{\pi L_{eff}}{d_c}\right)}{\frac{\pi L_{eff}}{d_c}} \ , \tag{4}$$

where L_{eff} is the effective length of the coil and d_c is the conductor diameter. The above formulation of the correction factor, K_s, has been originally introduced for the calculation of eddy current losses in the screened-rotor of an induction motor [24] and later adopted for the rotor retaining can of PM excited machines [25]. In our study, K_s is employed for calculating winding eddy current losses.

Another important reason for a possible overestimation of eddy current conductor losses by 2D methods may be attributed to not considering the magnetic field fringing and leakage, and hence neglecting the reduction of the flux density towards the ends, as illustrated in Fig. 9. Hybrid methods that employ 2D models ignore the fringing in the third dimension and typically result in larger and constant values of the flux density along an entire coil side. This is particularly important for machines with shorter stack length in the direction of effective length. Moreover, for axial flux machines the non-linear magnetic field along the radial direction can largely vary and sampling the flux density at only one particular diameter may not be truly representative of the flux density throughout the entire coil.

For an example AFPM machine, the magnitude of the flux density in each of the winding turns placed in the slot and surrounding a tooth was estimated with one sample per conductor using 2D and 3D models, respectively (Fig. 10). The 3D samples are taken for each of the 21 turns placed at equally distanced radial locations and then averaged. The 2D model was set-up for the mean diameter. The 2D model overestimation of the flux density, particularly for the turns that are closer to the top of the slot and closer to the teeth, is noticeable.

The coreless AFPM machine example from Fig. 11 is illustrative of the typical very large 3D variation of the flux density in the stator windings. In order to account for this, one solution would be to study multiple 2D models representative of slices at different radial coordinates and combine their contributions [26]. An increased number of 2D slices would increase, in principle, the accuracy of the simulation at the expense of increased computational time, but would not still account for the end field, which makes the use of 3D models worthwhile even more so.

IV. Proposed Method

The new method proposed in the paper employs a simplified 3D FE model with a single equivalent turn per coil as shown in Fig. 1a. The model is solved through transient analysis, however, it can be solved as a magnetostatic field problem or as an eddy current problem, but with an ideal zero conductivity set for the conductor. This is a suitable approach provided that induced field does not modify the source field, which is the case for resistance limited eddy current problems. Considering that in high performance electric machines the conductors are selected such that their dimensions are substantially lower than the skin depth, the problem is resistance limited and the eddy currents and their impact on the source field minimized. Inductance limited problems, wherein the induced eddy currents affect the source field, therefore, are only of theoretical interest in this context. The motivation for this approach is that the mesh required for satisfactorily accurate flux density calculations is substantially less dense than required for eddy current calculations in the winding conductors, resulting in faster solving and significantly lower computational resource requirements.

The method is developed for circular conductors, as such types are most commonly employed in electric machines, with multiple arrangements including form wound, precise tightly packed. In the case of rectangular wires, the dimensions are limited to certain values, and parallel wires like multiple strands in hand are not realistic.

Considering N_L sections in the radial direction and a precise winding configuration, as shown in Fig. 9:

$$
\begin{aligned}
&P_{n_\phi,n_z,n_L} = [x_n, y_n, z_n] \ ; \\
&n_\phi = 1, ...N_\phi \ ; \quad n_z = 1, ..., N_z \ ; \quad n_L = 1, ..., N_L \ ; \\
&x_n = \frac{ID}{2} \cos\left(\frac{\theta_{in}}{2}\right)\left(1 - \frac{n_L}{N_L}\right) + \frac{OD}{2} \cos\left(\frac{\theta_{on}}{2}\right)\frac{n_L}{N_L} \ ; \\
&y_n = \frac{ID}{2} \sin\left(\frac{\theta_{in}}{2}\right)\left(1 - \frac{n_L}{N_L}\right) + \frac{OD}{2} \sin\left(\frac{\theta_{on}}{2}\right)\frac{n_L}{N_L} \ ; \\
&\theta_{in} = \theta_i + 2\arcsin\left(\frac{d_c(2n_\phi - 1)}{ID}\right) \ ; \\
&\theta_{on} = \theta_o + 2\arcsin\left(\frac{d_c(2n_\phi - 1)}{OD}\right) \ ,
\end{aligned}
\tag{5}
$$

where P_{n_ϕ,n_z,n_L} are the Cartesian coordinates of the n^{th} point to be sampled for the flux density value; N_L, the number of sampling planes stacked in the direction of the effective length of the coil with an equal distance of $\Delta L = \frac{L_{eff}}{N_L}$ between them; N_ϕ and N_z, the number of turns in the circumferential and axial directions, respectively, as shown in Fig. 12a; ID and OD the inner and outer diameters; θ_i and θ_o the inner and the outer coil span angles, as illustrated in Fig. 12b.

It should be noted that for random windings, methods such as the one described in [3] maybe further developed for 3D application in conjunction with the new techniques described in this paper. Also, it is important to carefully adapt the flux density sampling to the problem. For example, if the real conductor dimensions are larger than the skin depth and the variations of flux density inside each conductor may be considerable, multiple flux samples in each plane are needed.

The eddy current losses for a circular conductor can be calculated based on a general analytical formulation:

$$
P_{eddy} = \frac{1}{R}\left(\frac{d\Phi}{dt}\right)^2 ; \quad dR = \frac{(L_{eff} + 2r)\rho}{\sqrt{\frac{d_c^2}{4} - r^2}\ dr} \ , \tag{6}
$$

where R is the resistance; Φ, the magnetic flux through the conductors; and ρ the conductor resistivity. Each conductor cross section can be divided into M segments as shown in Fig. 8. Assuming constant flux density for each segment, one field sample per segment may suffice.

Therefore, the eddy current loss for one coil side with $N_\phi \times N_z$ turns can be estimated as:

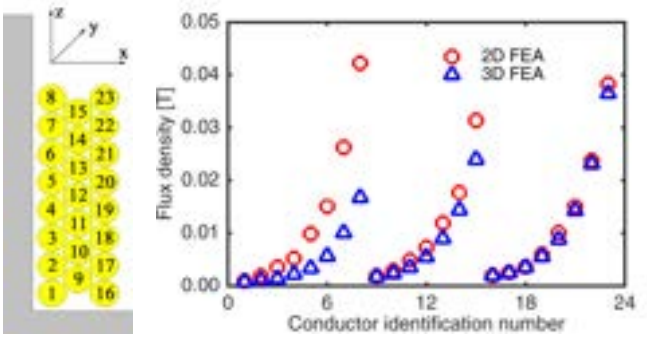

(a) (b)

Fig. 10: (a) Schematic of a coil side placed around the tooth displaying conductor identification numbers. (b) The flux density in each conductor, obtained by space sampling 2D and 3D FEA results, respectively. The 2D FEA typically results in an over estimation, especially for the conductors at the top slot and closest to the tooth.

$$
\begin{aligned}
&P_{eddy} = \frac{4L_{eff}^2}{\rho} \sum_{n_\phi=1}^{N_\phi} \sum_{n_z=1}^{N_z} \sum_{n=1}^{\infty} \sum_{m=1}^{M} ... \\
&\left[\left(\frac{d}{dt}\left(\frac{1}{L_{eff}} \int_{ID}^{OD} B_{m,n}\left(\frac{D}{2}, n_\phi, n_z\right)\ dD\right)\right)^2 \int_{r_{m1}}^{r_{m2}} \frac{r^2\sqrt{\frac{d_c^2}{4} - r^2}}{(L_{eff} + 2r)}\ dr\right] \\
&= \frac{L_{eff}}{2\rho} K_s \sum_{n_\phi=1}^{N_\phi} \sum_{n_z=1}^{N_z} \sum_{n=1}^{\infty} \sum_{m=1}^{M} ... \\
&\left[\left(\frac{d}{dt}\left(\frac{1}{L_{eff}} \int_{ID}^{OD} B_{m,n}(\frac{D}{2}, n_\phi, n_z)\ dD\right)\right)^2 (f(r_{m2}) - f(r_{m1}))\right] \ ; \\
&f(r) = r\sqrt{\frac{d_c^2}{4} - r^2}\ (2r^2 - \frac{d_c^2}{4}) + \left(\frac{d_c^2}{4}\right)^2 \arctan\frac{r}{\sqrt{\frac{d_c^2}{4} - r^2}} \ ,
\end{aligned}
\tag{7}
$$

where $B_{m,n}$ is the n^{th} harmonic of the flux density in the m^{th} section for the conductor associated with n_ϕ and n_z at the diameter D. The flux density of the m^{th} section includes the flux density of all sections that are inscribed in it (i.e. $B_m = \sum_{mi=1}^{m} B_{mi}$).

If the conductors are sufficiently small, the flux density throughout the conductor cross section may be assumed constant. Taking the variation of B along the effective length from inner to outer diameter into account, and neglecting the harmonics content, the eddy current losses of the machine with N_c coil sides are derived as:

$$
\begin{aligned}
P_{eddy} = &\frac{\pi L_{eff} N_c d_c^4 \omega_e^2 K_s}{128\rho} ... \\
&\sum_{n_\phi=1}^{N_\phi} \sum_{n_z=1}^{N_z} \left[\frac{1}{L_{eff}} \int_{ID}^{OD} B\left(\frac{D}{2}, n_\phi, n_z\right)\ dD\right]^2 .
\end{aligned}
\tag{8}
$$

A discrete sampling along radial direction with N_L samples can be performed in which case the coordinates of the sample points in the general 3D FEA model can be obtained from (5).

TABLE I: ADDITIONAL AC COPPER LOSSES IN THE WINDINGS DUE TO EDDY CURRENTS, CALCULATED WITH DIFFERENT FEA AND HYBRID METHODS FOR OPEN-CIRCUIT AND FULL LOAD OPERATING CONDITIONS.

AFPM machine	Eddy current loss	**3D FEA**	**Hy-3D**	**2D FEA**	**Hy-2D**
Coreless	Open-circuit [W]	420.5	424.0	611.7	520.3
Open-slot machine	Open-circuit [W]	35.7	36.7	41.4	39.5
Open-slot machine	Full load [W]	44.7	48.5	57.0	49.4
Approximate FEA computational time		37 hours	35 minutes	2 minutes	12 seconds

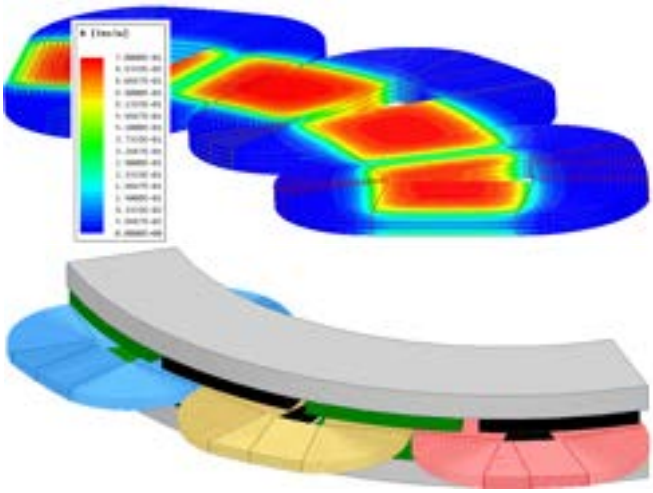

Fig. 11: The magnetic flux density in the conductors of an example AFPM coreless machine calculated with 3D FEA. For such machines, the winding is directly exposed to the airgap field, the magnitude and multi-dimensional variation of which can be substantial, resulting in significant eddy current losses.

Both (7) and (8) assume that within the coil side the largest eddy current flow path follows the entire active length of the coil with shorter paths being possible, as shown in Fig. 13. The following equation, in which different eddy current paths inside one conductor are specified with the index k, takes this effect into consideration:

$$P_{eddy} = \frac{\pi L_{eff} N_c d_c^4 \omega_e^2 K_s}{128\rho} \sum_{n_\phi=1}^{N_\phi} \sum_{n_z=1}^{N_z} \sum_{k=1}^{k_{max}} C_k \cdot B_{path,k}^{\,2} \ , \tag{9}$$

where C_k is the coefficient adjusting the resistance of each current path and $B_{path,k}$ is the flux density within the k^{th} current path. In the case of an odd number of samples, N_L, along the coil side:

$$\begin{aligned} k_{max} &= \frac{N_L+1}{2} \ , \quad C_k = \frac{2+4(k-1)}{N_L} \ , \\ B_{path,k} &= \frac{1}{1+2(k-1)} \sum_{i=\frac{N_L+1}{2}-(k-1)}^{\frac{N_L+1}{2}+(k-1)} B_i \ . \end{aligned} \tag{10}$$

For an even number of samples:

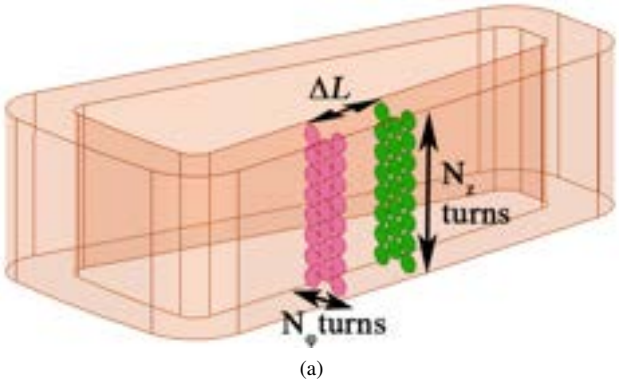

(a)

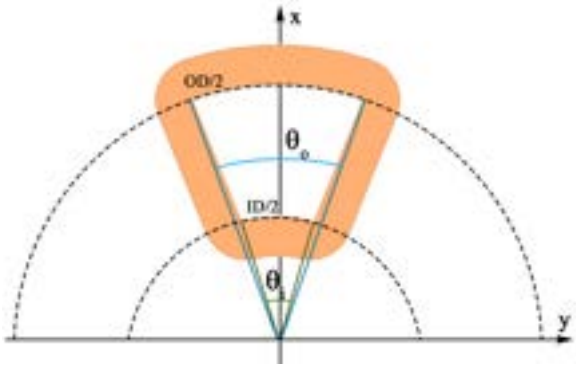

(b)

Fig. 12: (a) The flux density sampling planes employed by the new hybrid 3D FEA method stacked in the direction of the main current flow. (b) Three-dimensional sampling is performed also in order to take end effects into account. The axial cross section schematic depicts the coil span and the in inner and outer diameter as used in (5).

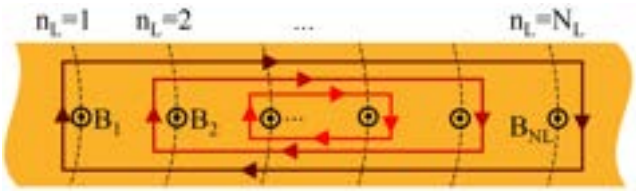

Fig. 13: Eddy current paths with different length along the coil side.

$$\begin{aligned} k_{max} &= \frac{N_L}{2} \ , \quad C_k = \frac{4k}{N_L} \ , \\ B_{path,k} &= \frac{1}{2k} \sum_{i=\frac{N_L}{2}-(k-1)}^{\frac{N_L}{2}+k} B_i \ . \end{aligned} \tag{11}$$

In principle, the proposed method can be developed and

applied for wires with a rectangular cross section. Nevertheless, this may be of lesser practical interest, because such wires typically have larger dimensions, and hence the main assumption of constant flux density within a conductor may no longer hold. A solution would be to consider multiple field samples for each wire cross section in both directions. The implementation of such an approach would be complex and require an additional stage for post-processing on yet another discretization grid, which would preferably be rectangular and would still need to be coordinated with the electromagnetic FE triangulation that yields the $B_{a\phi}$ and B_{az} flux density components. The full mathematical development exceeds the space limitations of the current paper and the corresponding principles are only summarized in the following.

For the case of a rectangular wire, (7) can be rewritten as:

$$P_{eddy} = \frac{L_{eff}}{2\rho} K_s \sum_{n_\phi=1}^{N_\phi} \sum_{n_z=1}^{N_z} \sum_{n=1}^{\infty} \left(p_{eddy,w} + p_{eddy,h}\right) \ , \tag{12}$$

where $p_{eddy,w}$ and $p_{eddy,h}$ are used to distinguish eddy current loss as a result of flux density components in circumferential and axial directions. These can be estimated as:

$$p_{eddy,w} = \sum_{m_w=1}^{M_w} \left(\frac{d}{dt} \left(\frac{1}{L_{eff}} \int_{ID}^{OD} B_{m_w,n} \left(\frac{D}{2}, n_\phi, n_z \right) \ dD \right) \right)^2 ... \\ \frac{h}{3} \left(w_{m2}^3 - w_{m1}^3 \right) \ , \tag{13}$$

and

$$p_{eddy,h} = \sum_{m_h=1}^{M_h} \left(\frac{d}{dt} \left(\frac{1}{L_{eff}} \int_{ID}^{OD} B_{m_h,n} \left(\frac{D}{2}, n_\phi, n_z \right) \ dD \right) \right)^2 ... \\ \frac{w}{3} \left(h_{m2}^3 - h_{m1}^3 \right) \ , \tag{14}$$

where M_w and M_h are the number of samples per conductor cross section along the width and height of the cross section, $B_{m_w,n}$ and $B_{m_h,n}$ represent the n^{th} harmonic of the flux density in m_w^{th} and m_h^{th} section, respectively. In a similar approach to the one introduced for circular wires, the flux density of the m^{th} section includes all the sections that are inscribed in it.

Following this approach, the proposed 3D hybrid method would require $M_w \times M_h \times N_\phi \times N_z \times N_L$ sampling points. Although in principle this is possible substantial efforts are required for implementation. The main objective of the current paper is top focus within the space-limitations on the far more widely used circular wires, which can be very thin in order to minimize eddy current AC losses, and hence only one sample per conductor is typically sufficient as illustrated by the numerical studies presented in the following section.

V. Validation of the Proposed Method

The proposed method is verified for a 24-slot 20-pole, axial flux machine with open slots. Open slot machines and tend to feature larger flux leakage, conductor eddy currents and additional copper loss. The turns located on top of the slot experience larger flux density and hence have higher loss. Therefore each turn has a separate B_a which may not be uniformly distributed, necessitating separate calculation and data sampling for each turn as shown in Fig. 10. The four calculation methods considered are:

- **3D FEA**: time-transient 3D FEA with detailed turn-by-turn, i.e., wire-by-wire, representation of the winding coils (considered the most accurate method),
- **Hy-3D**: the new hybrid method with samples of flux density obtained from a simplified 3D model (the proposed method),
- **2D FEA**: time-transient 2D FEA with turn-by-turn wire-by-wire representation of the winding coils,
- **Hy-2D**: a hybrid method with samples from a simplified 2D FEA.

An example mesh plot used with the first method, the detailed time-stepping 3D FEA, is presented in Fig. 14. The hybrid methods studied, i.e., Hy-3D and Hy-2D , employed time-transient analysis. Nevertheless, in principle magneto-static analysis and adaptive meshing may also be used, which could further reduce the computational time.

The results for different methods are presented in Table I and include only the additional ac induced eddy current losses in the windings and not the steady-state dc-type loss component due to the main supply current. In Table I, the first method listed, the 3D FEA, validated through measurements in Section II, is considered as the most accurate approach and its results serve as reference. The estimation differences for the Hy-3D, 2D FEA, and Hy-2D methods are 3%, 16%, and 11% at open-circuit, respectively and 8%, 28%, and 11% on load, respectively, illustrating the advantages of the new Hy-3D method in terms of satisfactory estimation.

The results show increase in the additional winding loss for load operating conditions. This is because the varying flux density not only originates from magnets, but also the ac current flowing in the coil. The input armature winding current density of the under study air cooled cored AFPM machine is about 1.5 A/mm^2, however, due to eddy currents, at full load it increases to about 9.5 A/mm^2 peak. At open-circuit the current density is solely due to eddy currents and is about 6.5 A/mm^2, that is the peak current density at fundamental frequency of 1.6 kHz. Therefore, the majority of eddy currents for this case study is due to PM passing over the winding. At loads significantly higher than rated values, additional care may be needed to ensure negligible proximity losses. Another reason for higher ac copper losses at load can be attributed to the increased variation of the flux density due to armature reaction, causing distortion and asymmetry in flux lines.

The results of the proposed method are in agreement with detailed 3D FEA in load operation as well as open-circuit. Considering that the proposed method does not take into account the possible skin losses and proximity due to neighboring conductors, the satisfactory agreement between results attests to a significantly higher PM flux contribution to the ac copper losses and negligible proximity losses in the case studies.

For a further verification of the efficacy of the proposed method, it is also implemented on a coreless AFPM machine

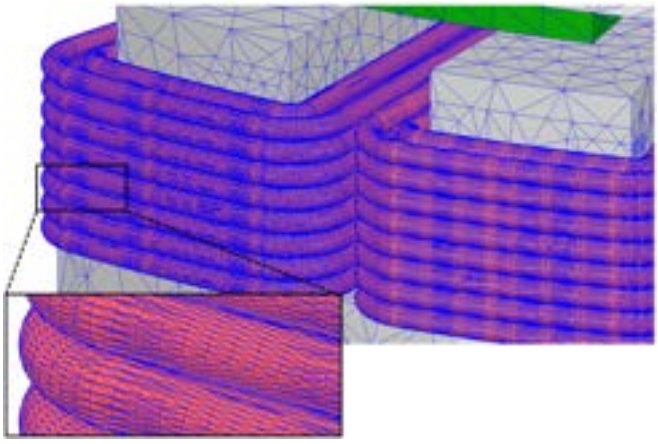

Fig. 14: The 3D mesh plot for the turn-by-turn model of the AFPM machine with open slots.

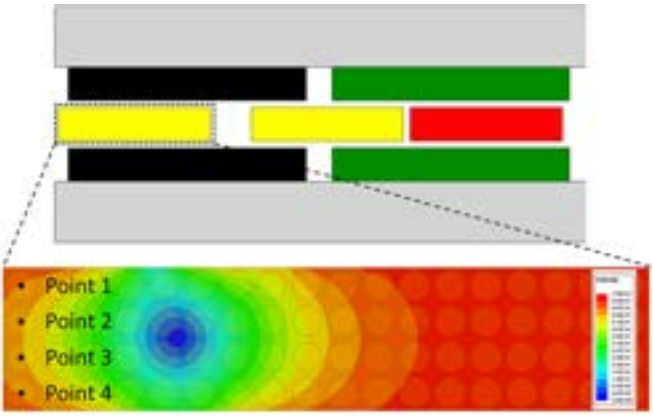

Fig. 15: The general 2D model for sampling flux density values employed in the hybrid method. The coil cross section marked with dashed box is zoomed in to show the location of four sampling points in the center of round conductors.

with 12 coils and 16 poles, as shown in Fig. 11. Coreless PM machines are attractive options for high speed applications due to the elimination of the stator core loss. On the other hand, all the conductors are exposed to the air-gap flux density hence have larger eddy currents, which is more critical at higher speeds. This forces the application of thinner conductors and a larger number of turns and strands, necessitating the consideration of expensive Litz wires. Therefore the estimation of ac copper loss in the design stage in air-cored machine topologies is of utmost importance.

Due to the axial symmetry shown in Fig. 15 and Fig. 16 the flux density observed by points 1 and 4, and also points 2 and 3 are the same. Furthermore, due to the rotation of the rotor, modeling the flux density variation with time for a single column of turns is sufficient. This indicates that modeling only 2 turns may suffice. This is especially interesting in case of the detailed and computationally expensive FEA models [23]. Considerable reduction in computational efforts and mesh size (90% less number of mesh elements) is achieved by modeling only two turns for the coreless machine case study without affecting the accuracy of the results.

It is observed that the additional eddy current losses calculated for the coreless machine example are significantly larger compared with the example open slot machine since the windings in the former are exposed to the fundamental air-gap flux density. The results show that the losses predicted by the Hy-3D method are in close agreement with 3D FEA (Table I). It should be noted that for the coreless machine studied, the 2D based methods do not provide accurate estimations.

The new Hy-3D method is faster by one order of magnitude than the reference full 3D FEA and it is applicable for a wide range of problems. Another advantage, as compared with 2D formulations, which are typically faster, is that the proposed hybrid method should be more accurate as it takes into account the effect of end turns by considering both the return path of eddy currents and also the variation in flux throughout the effective length of the coils. The correction factor, K_s, introduced in (4), for the considered example machines is

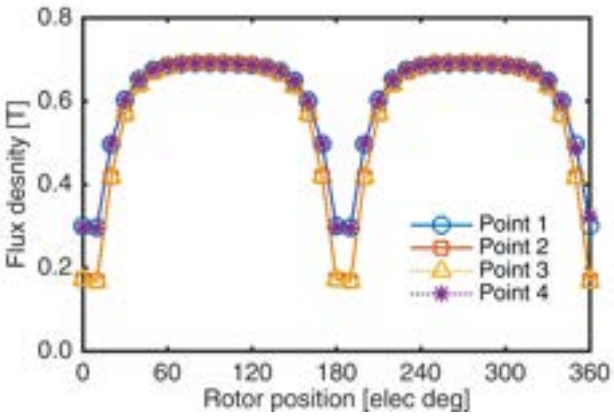

Fig. 16: The flux density in the sampling points shown in Fig. 15 at different time steps.

0.98 in both cases, meaning that the correction due to the end winding is minimal and the differences in results between methods may be substantially associated with the 3D field variation along the active sides of the coils.

It may be noted that such approaches for reducing the modeling efforts are applicable for eddy current loss calculation at open-circuit or cases where proximity effects are not considerable and the eddy losses are mostly caused by the magnet flux.

VI. Conclusion

This paper studies numerical, analytical and hybrid methods for the calculation of ac losses in the stator conductors of axial flux machines due to the open-circuit field generated by the rotor permanent magnets. In order to minimize such losses, which can be otherwise significant, systematic design optimization is required. The process typically involves a very large number of candidate designs and thus, there is a need for a fast method to accurately evaluate these losses. The proposed hybrid analytical-FEA method provides a solution in this respect.

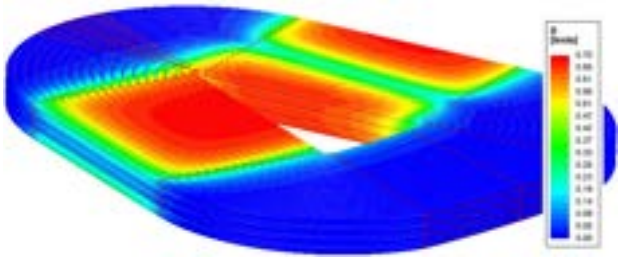

(a)

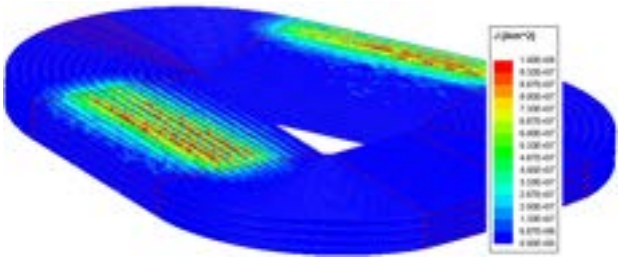

(b)

Fig. 17: (a) Flux density obtained from the 3D FEA model of the coreless machine case study, illustrating the lower values closer to the end turns. (b) The current density distribution.

The computational results for two different types of AFPM machines show that the new method is superior to other hybrid FE techniques in terms of accuracy and that its results satisfactorily compare with reference detailed 3D FEA, while reducing the computational time by one order of magnitude. The new method achieves a trade-off between speed and precision, making it suitable for different stages of the design process of an electrical machine.

ACKNOWLEDGMENT

The support of National Science Foundation NSF Grant #1809876, of University of Kentucky, the L. Stanley Pigman endowment, and of ANSYS Inc. is gratefully acknowledged.

REFERENCES

[1] M. Rosu, P. Zhou, D. Lin, D. M. Ionel, M. Popescu, F. Blaabjerg, V. Rallabandi, and D. Staton, *IEEE Press Series on Power Engineering*. IEEE, 2018. [Online]. Available: https://ieeexplore-ieee-org.ezproxy.uky.edu/document/8233737

[2] M. Popescu and D. G. Dorrell, "Proximity losses in the windings of high speed brushless permanent magnet ac motors with single tooth windings and parallel paths," *IEEE Transactions on Magnetics*, vol. 49, no. 7, pp. 3913–3916, July 2013.

[3] A. Fatemi, D. M. Ionel, N. A. O. Demerdash, D. A. Staton, R. Wrobel, and Y. C. Chong, "A computationally efficient method for calculation of strand eddy current losses in electric machines," in *2016 IEEE Energy Conversion Congress and Exposition (ECCE)*, Sep. 2016, pp. 1–8.

[4] C. R. Sullivan, "Optimal choice for number of strands in a litz-wire transformer winding," *IEEE Transactions on Power Electronics*, vol. 14, no. 2, pp. 283–291, March 1999.

[5] P. H. Mellor, R. Wrobel, and N. McNeill, "Investigation of proximity losses in a high speed brushless permanent magnet motor," in *Conference Record of the 2006 IEEE Industry Applications Conference Forty-First IAS Annual Meeting*, vol. 3, Oct 2006, pp. 1514–1518.

[6] L. J. Wu and Z. Q. Zhu, "Simplified analytical model and investigation of open-circuit ac winding loss of permanent-magnet machines," *IEEE Transactions on Industrial Electronics*, vol. 61, no. 9, pp. 4990–4999, Sept 2014.

[7] D. C. Hanselman and W. H. Peake, "Eddy-current effects in slot-bound conductors," *IEE Proceedings - Electric Power Applications*, vol. 142, no. 2, pp. 131–136, March 1995.

[8] C. R. Sullivan, "Computationally efficient winding loss calculation with multiple windings, arbitrary waveforms, and two-dimensional or three-dimensional field geometry," *IEEE Transactions on Power Electronics*, vol. 16, no. 1, pp. 142–150, Jan 2001.

[9] L. J. Wu and Z. Q. Zhu, "Analytical investigation of open-circuit eddy current loss in windings of pm machines," in *2012 XXth International Conference on Electrical Machines*, Sep. 2012, pp. 2759–2765.

[10] P. Zhang, G. Y. Sizov, J. He, D. M. Ionel, and N. A. O. Demerdash, "Calculation of magnet losses in concentrated-winding permanent-magnet synchronous machines using a computationally efficient finite-element method," *IEEE Transactions on Industry Applications*, vol. 49, no. 6, pp. 2524–2532, Nov 2013.

[11] M. R. Shah and A. M. EL-Refaie, "Eddy-current loss minimization in conducting sleeves of surface pm machine rotors with fractional-slot concentrated armature windings by optimal axial segmentation and copper cladding," *IEEE Transactions on Industry Applications*, vol. 45, no. 2, pp. 720–728, March 2009.

[12] P. B. Reddy, T. M. Jahns, and T. P. Bohn, "Modeling and analysis of proximity losses in high-speed surface permanent magnet machines with concentrated windings," in *2010 IEEE Energy Conversion Congress and Exposition*, Sep. 2010, pp. 996–1003.

[13] P. Mellor, R. Wrobel, D. Salt, and A. Griffo, "Experimental and analytical determination of proximity losses in a high-speed pm machine," in *2013 IEEE Energy Conversion Congress and Exposition*, Sep. 2013, pp. 3504–3511.

[14] D. A. Gonzalez and D. M. Saban, "Study of the copper losses in a high-speed permanent-magnet machine with form-wound windings," *IEEE Transactions on Industrial Electronics*, vol. 61, no. 6, pp. 3038–3045, June 2014.

[15] I. Petrov, M. Polikarpova, P. Ponomarev, P. Lindh, and J. Pyrhönen, "Investigation of additional ac losses in tooth-coil winding pmsm with high electrical frequency," in *2016 XXII International Conference on Electrical Machines (ICEM)*, Sept 2016, pp. 1841–1846.

[16] A. Al-Timimy, P. Giangrande, M. Degano, M. Galea, and C. Gerada, "Investigation of ac copper and iron losses in high-speed high-power density PMSM," in *2018 XIII International Conference on Electrical Machines (ICEM)*, Sept 2018, pp. 263–269.

[17] N. Aliyu, G. Atkinson, N. Stannard, and M. Kimiabeigi, "Assessment of AC copper loss in permanent magnet axial flux machine with soft magnetic composite core," in *2018 IX International Conference on Power Electronics Machines and Drives (PEMD)*, Apr 2018.

[18] G. Volpe, M. Popescu, F. Marignetti, and J. Goss, "Modelling ac winding losses in a pmsm with high frequency and torque density," in *2018 ECCE*, Sept 2018, pp. 2300–2305.

[19] O. A. Mohammed and S. Ganu, "FE-circuit coupled model of electric machines for simulation and evaluation of EMI issues in motor drives," *IEEE Transactions on Magnetics*, vol. 46, no. 8, pp. 3389–3392, Aug 2010.

[20] N. Taran, V. Rallabandi, D. M. Ionel, G. Heins, and D. Patterson, "A comparative study of methods for calculating ac winding losses in permanent magnet machines," in *2019 IEEE International Electric Machines Drives Conference (IEMDC)*, 2019, pp. 2265–2271.

[21] N. Taran and D. M. Ionel, "A hybrid analytical and fe-based method for calculating ac eddy current winding losses taking 3d effects into account," in *2019 IEEE Energy Conversion Congress and Exposition (ECCE)*, 2019, pp. 4867–4872.

[22] *ANSYS Electronics Desktop, version 19.1*, 2019.

[23] G. Heins, D. M. Ionel, D. Patterson, S. Stretz, and M. Thiele, "Combined experimental and numerical method for loss separation in permanent-magnet brushless machines," *IEEE Transactions on Industry Applications*, vol. 52, no. 2, pp. 1405–1412, March 2016.

[24] R. L. Russell and K. H. Norsworthy, "Eddy currents and wall losses in screened-rotor induction motors," *Proceedings of the IEE - Part A: Power Engineering*, vol. 105, no. 20, pp. 163–175, April 1958.

[25] J. R. Hendershot and T. J. E. Miller, *Design of brushless permanent-magnet motors / J.R. Hendershot, Jr., T.J.E. Miller*. Magna Physics Pub. ; Clarendon Press Hillsboro, OH : Oxford, 1994.

[26] R.-J. Wang and M. J. Kamper, "Calculation of eddy current loss in axial field permanent-magnet machine with coreless stator," *IEEE Transactions on Energy Conversion*, vol. 19, no. 3, pp. 532–538, Sep. 2004.